

# The Reduction Analysis of Bearing Capacity of the Footing Near Excavations in the Loess Area

Qi Zhang<sup>1</sup>, Xiaoyan Lin<sup>1,2</sup>, Aoxin Li<sup>1</sup>

<sup>1</sup> School of Earth Sciences and Engineering, Xi'an Shiyou University, Xi'an Shaanxi, 710065, China

<sup>2</sup> Shaanxi Key Laboratory of Petroleum Accumulation Geology, Xi'an Shiyou University, Xi'an Shaanxi, 710065, China

## Abstract

With the increasing development of urban underground space, the impact of foundation pit excavation on adjacent buildings has become a prominent issue. Based on extensive statistical parameters of loess regions and numerical simulations using Geo-Slope, this study analyzes the reduction pattern of the ultimate bearing capacity of adjacent strip foundations under unsupported excavation conditions. The research focuses on the influence of excavation depth ( $H$ ), distance from the foundation to the pit edge ( $L$ ), and building width ( $B$ ) on the reduction of foundation bearing capacity ( $p_u$ ). A reduction factor ( $K$ ) is introduced. The results show that  $p_u$  gradually decreases with increasing  $H$  and  $B$ , and decreases with decreasing  $L$ . Moreover,  $K$  decreases as  $\lambda$  ( $\lambda=L/H$ ) increases.

## Keywords

Loess; Excavation; The Foundation Bearing Capacity; Finite Element; Reduction Factor.

## 1. Introduction

With the continuous expansion of urban construction into underground spaces, foundation pit engineering has gradually become a critical component of urban geological engineering. In loess regions, ground disturbance caused by excavation has emerged as an increasingly prominent issue, particularly regarding its impact on the bearing capacity of adjacent existing building foundations, which poses a significant challenge in engineering construction [1-4]. Current domestic and international research primarily focuses on surface settlement, deformation mechanisms of foundation pit sidewalls, and calculation methods for foundation bearing capacity [5-8]. However, studies on the reduction of foundation bearing capacity near excavations mostly rely on traditional Terzaghi's calculation method, with limited application of finite element analysis to investigate the influence of various factors. Based on the geological characteristics of typical loess regions, this paper employs Geo-Slope software for simulation to systematically study the reduction patterns of ultimate bearing capacity for strip foundations under the influence of multiple factors during unsupported excavation. The findings aim to provide theoretical reference for urban engineering projects under similar geological conditions.

## 2. Foundation Characteristics in Loess Regions and Features of Excavation

### 2.1. Engineering Properties of Loess

The loess region in China can be divided into four major zones based on the variation patterns of foundation bearing capacity and its main influencing factors: the Eastern Region, the Guanzhong Plain Region, the Longdong-Northern Shaanxi and Western Shanxi Region, and the

Longxi Region [9-11]. The ranges of physical and mechanical indices and bearing capacity are presented in Table 1.

**Table 1.** Physical and Mechanical Indicators and Bearing Capacity of Four Major Loess Regions

Region	%	KN·m <sup>-3</sup>	l <sub>v</sub> /%	I <sub>p</sub>	e	δ <sub>ζ</sub>	p <sub>u</sub> / kPa
the Eastern Region	6~24	14.0~19.0	23~33	8~13	0.60~1.31	0.015~0.08	180~260
the Guanzhong Plain Region	11~28	14.0~18.0	23~32	9~13	0.94~1.21	0.029~0.080	170~230
the Longdong-Northern Shaanxi and Western Shanxi Region	9~24	14.0~17.0	20~31	7~13	0.80~1.20	0.019~0.088	160~210
he Longxi Region	3~25	12.0~18.0	21~31	4~12	0.70~1.30	0.020~0.220	150~230

### 2.2. Characteristics of Foundation Pit Excavation

As shown in Figure 1, the unloading process during excavation can be divided into two stress paths: vertical unloading (Path F) and horizontal unloading (Path B). Vertical unloading reduces the vertical stress in the soil at the pit bottom, leading to rebound and heaving of the pit base. Horizontal unloading results in the release of lateral stress, causing the retaining wall to displace inward toward the pit. Due to the non-uniform displacement of the wall, the earth pressure in the active zone outside the pit exhibits a nonlinear distribution. Furthermore, because of the soil arching effect, the lateral pressure behind the wall tends to become more uniform. The wall displacement induces deformation in the surrounding soil, generating displacement-compatible deformation and additional stresses at the soil-structure interface. Plastic zones develop in the corner regions of the pit and within the passive zone. The deformation propagates to the ground surface through soil rheology, resulting in surface settlement and potential damage to adjacent structures[12-16].

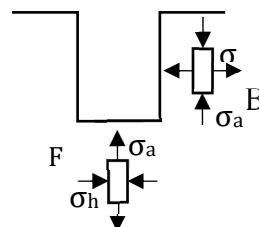


**Fig 1.** Excavation Unloading Path Diagram

## 3. Selection of Foundation Bearing Capacity Calculation Methods

### 3.1. Terzaghi's Ultimate Bearing Capacity Theory

Figure 2 illustrates the calculation model for Terzaghi's theory, which is based on the following assumptions [17-20]:

- 1) Perfectly Rough Base: Full friction develops between the foundation base and the soil, forming an elastic wedge.
- 2) Fixed Shape of Failure Surface: The slip surface consists of a logarithmic spiral segment bc and a straight-line segment cd. The passive zone acd satisfies an inclination angle of  $45^\circ - \varphi/2$ .
- 3) Neglect of Strength of Overlying Soil above the Base: The overburden is replaced by a uniformly distributed surcharge load  $q = \gamma D$ .

The general expression for this approximate solution is:

$$P_u = cN_c + \frac{\gamma B}{2} N_\gamma + \gamma D N_q$$

$N_c$ ,  $N_\gamma$  and  $N_q$  are the bearing capacity factors:

$$N_q = \tan^2 \left( 45^\circ + \frac{\varphi}{2} \right) e^{\pi \tan \varphi}$$

$$N_\gamma = 2 \operatorname{tg} \varphi \left[ \tan^2 \left( 45^\circ + \frac{\varphi}{2} \right) e^{\pi \tan \varphi} + 1 \right]$$

$$N_c = \operatorname{cot} \varphi \left[ \tan^2 \left( 45^\circ + \frac{\varphi}{2} \right) e^{\pi \tan \varphi} - 1 \right]$$

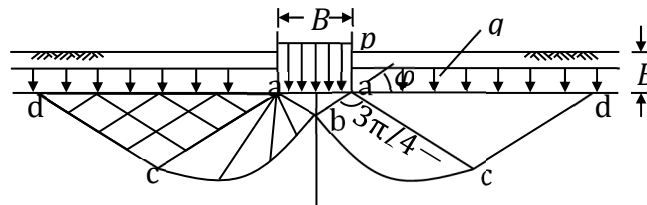


**Fig 2.** Theoretical Calculation Diagram Based on Terzaghi's Theory

### 3.2. Finite Element Analysis Method

For investigating the ultimate bearing capacity of heterogeneous media under external loads, the finite element method serves as a highly effective numerical analysis approach [20-22]. In this study, Geo-slope software is employed to establish a model that simulates the mechanical behavior of loess based on the Mohr-Coulomb constitutive criterion. The potential slip surface is identified by calculating the minimum safety factor ( $F_s$ ) at any point. The corresponding load ( $p$ ) when  $F_s = 1$  is taken as the ultimate bearing capacity ( $p_u$ ). This method, which enables dynamic simulation of stress redistribution and plastic zone development during excavation unloading and accurately captures the configuration of slip surfaces, is more suitable for analyzing heterogeneous loess compared to traditional theoretical methods.

$$F_s = \frac{\sqrt{(\sigma_1 \cdot \tan \varphi + c) \cdot (\sigma_3 \cdot \tan \varphi + c)}}{\frac{\sigma_1 - \sigma_3}{2}}$$

### 3.3. Selection of the Method

**Table 2.** Calculation Results Using Conventional Methods

$\varphi(^{\circ})$	$\operatorname{cot} \varphi$	$\tan(45^\circ + \varphi/2)$	$\pi \tan \varphi$	$N_c$	$p_u/\text{kPa}$
14	4.01	1.28	0.78	10.32	186
15	3.73	1.3	0.84	10.87	196
16	3.48	1.33	0.9	11.66	210
17	3.27	1.35	0.96	12.29	221
18	3.08	1.38	1.02	13.19	237

**Table 3.** Calculation Results Using Finite Element Method

Category	Value				
$\varphi(^{\circ})$	14	15	16	17	18
$N_c$	10.06	11.11	11.67	12.5	13.33
$p_u/\text{kPa}$	190	200	210	225	240

To compare the Terzaghi calculation method with the finite element method, a representative foundation is examined. By neglecting the unit weight of the soil and the effects of excavation, the bearing capacity is calculated using both the Terzaghi method and the finite element method, respectively. The calculation results are presented in Tables 2 and 3. The results obtained from the two methods are in good agreement. Considering that the finite element

method is both convenient and accurate, it is selected in this study for determining and analyzing the foundation bearing capacity.

## 4. Reduction Analysis of Foundation Bearing Capacity for Existing Buildings due to Excavation

### 4.1. Model Establishment

The geometric model is shown in Figure 3, with key parameters being the excavation depth  $H$ , the building foundation width  $B$ , the distance between the foundation and the excavation edge  $L$ , and the foundation depth  $D$ . The foundation depth is assumed to be  $D = 0$  m. When analyzing the influence of the building width  $B$ , different definitions of  $L$  lead to different analytical approaches, as illustrated in Figure 4. Here,  $L1$  represents the distance from the excavation edge to the building edge, while  $L2$  represents the distance from the excavation edge to the center of the building foundation.

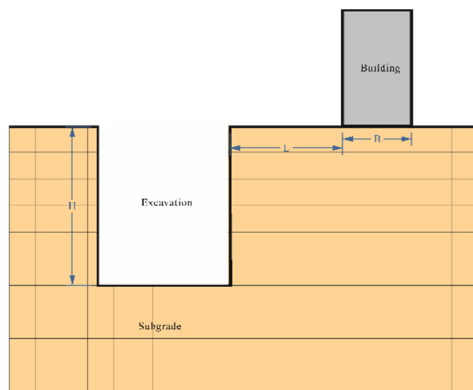


Fig 3. Computational Geometric Model

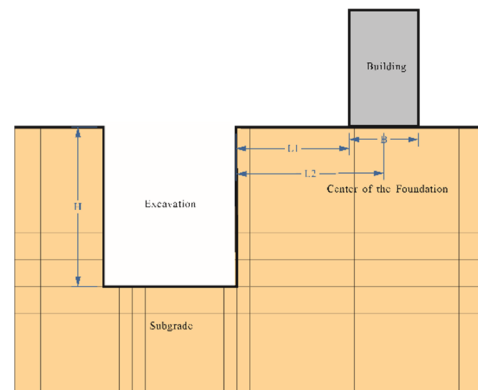


Fig 4. Different  $L$  Values in Foundation Width Influence Analysis

### 4.2. Influence Analysis

This study focuses on the influence of unsupported loess excavation on the bearing capacity of adjacent building foundations. To ensure the stability of the excavation, the excavation depth  $H$  must be strictly limited. The ultimate permissible value of  $H$  varies depending on different values of the soil's internal friction angle  $\varphi$  and cohesion  $C$ . This paper primarily considers the case where the cohesion  $C$  is taken as 18 kPa. With an internal friction angle  $\varphi$  of  $17^\circ$ , the excavation fails when  $H$  exceeds 7 m; therefore, the maximum value of  $H$  is set at 7 m.

As can be seen from Figures 5 and 6, the foundation bearing capacity  $p_u$  gradually decreases with increasing excavation depth  $H$ ; however, the trend of change in  $p_u$  differs for different values of unit weight  $\gamma$  and  $\varphi$ . Figures 7 and 8 show that  $p_u$  decreases as the excavation distance  $L$  decreases. Figure 9 indicates that when  $L1$  is constant and the building foundation width  $B$  is relatively small,  $p_u$  decreases as  $B$  increases. Furthermore, the rate of decrease in  $p_u$  diminishes with increasing  $B$ , eventually stabilizing. As shown in Figure 10,  $p_u$  decreases with increasing foundation width  $B$  when  $L2$  is constant.

In engineering practice, the foundation width  $B$  is unlikely to be very small; therefore, its influence on  $p_u$  is negligible. Consequently, this study only discusses the influence of  $L$  and  $H$  on the post-excavation bearing capacity of building foundations. Definition: The foundation bearing capacity without excavation is denoted as  $p_{u0}$ . The foundation bearing capacity after excavation is denoted as  $p_u$ .  $K$  is defined as the reduction coefficient, with  $\lambda = L / H$ , and  $K = (p_{u0} - p_u) / p_{u0}$ . The variation of the reduction coefficient  $K$  with  $\lambda$  differs under different conditions. Two cases are considered separately: when  $H$  is constant and when  $L$  is constant.

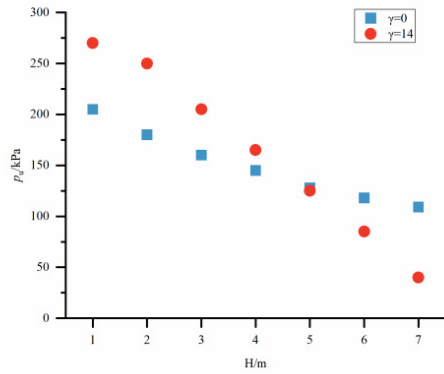


**Fig 5.** Variation Curve of  $p_u$  with Excavation Depth  $H$

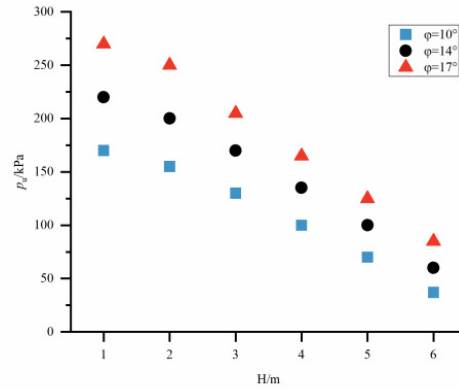


**Fig 6.** Variation Curve of  $p_u$  with Excavation Depth  $H$  under Different  $\phi$

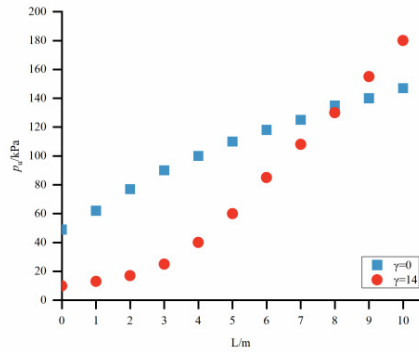


**Fig 7.** Variation Curve of  $p_u$  with Excavation Distance  $L$  under Different  $\gamma$

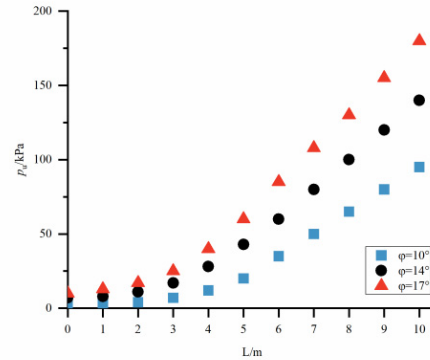


**Fig 8.** Variation Curve of  $p_u$  with Excavation Distance  $L$  under Different  $\phi$

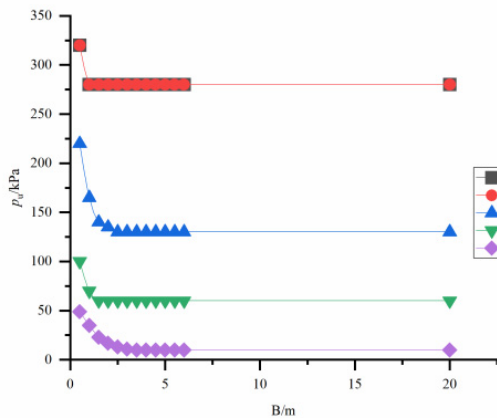


**Fig 9.** Variation Curve of Foundation Bearing Capacity  $p_u$  with  $B$  under Different  $L_1$  Values (with  $L_1$  Fixed)

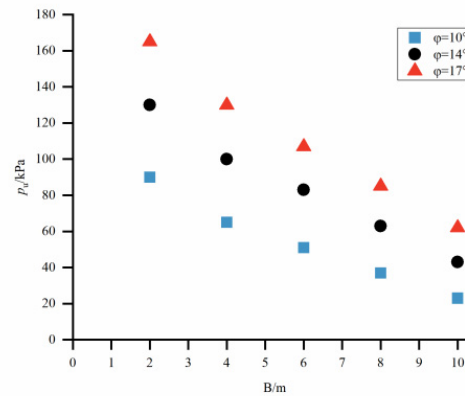


**Fig 10.** Variation Curve of Foundation Bearing Capacity  $p_u$  with  $B$  under Different  $\phi$  Values ( $L_2 = 10$ )

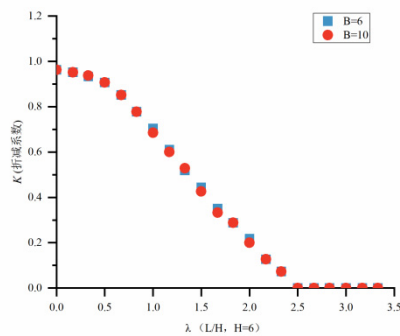


**Fig 11.** Variation Curve of  $K$  (Reduction Factor) with  $\lambda$  ( $L/H$ ,  $H = 6$ )

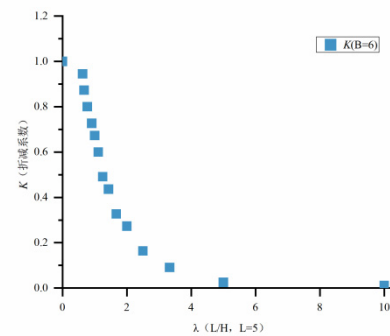


**Fig 12.** Variation Curve of  $K$  (Reduction Factor) with  $\lambda$  ( $L/H$ ,  $L = 5$ )

Figures 11 and 12 present the curves of the reduction coefficient  $K$  versus  $\lambda$ . It can be observed from the figures that the reduction coefficient  $K$  decreases as  $\lambda$  increases.

## 5. Conclusion

This paper employs an elastoplastic finite element method to analyze the reduction patterns of the ultimate bearing capacity of adjacent strip foundations under various influencing factors during unsupported excavation. The preliminary conclusions are as follows:

- (1) When the distance between the excavation and the building ( $L$ ) and the foundation width ( $B$ ) are constant, the ultimate bearing capacity of the foundation ( $p_u$ ) decreases as the excavation depth ( $H$ ) increases. The influence of  $H$  on  $p_u$  is relatively minor when the excavation depth is shallow; however, as the excavation deepens, the effect of  $H$  on  $p_u$  becomes significantly more pronounced.
- (2) When the excavation depth ( $H$ ) and foundation width ( $B$ ) are constant, the ultimate bearing capacity of the foundation ( $p_u$ ) decreases as the distance  $L$  decreases. Moreover, the reduction in  $p_u$  becomes more pronounced with smaller values of  $L$ .
- (3) When the distance  $L$  and excavation depth  $H$  are constant, the ultimate bearing capacity of the foundation ( $p_u$ ) decreases with an increase in foundation width ( $B$ ) when  $B$  is very small. However, once the distance  $L$  reaches a certain magnitude, the influence of foundation width  $B$  on  $p_u$  can be neglected.
- (4) When the foundation width ( $B$ ) is constant, the reduction coefficient ( $K$ ) varies at different rates with changes in  $\lambda$ , yet the overall trend remains consistent:  $K$  decreases as  $\lambda$  increases.

## Acknowledgments

Funding Project: Theoretical and Experimental Research on Strength of Unsaturated Loess Based on Absorptive Stress (No. 41402274).

## References

- [1] Zheng X, Tang J X, Cheng Y C, et al. Influence of whole process of deep foundation pit construction of subway station on adjacent buildings in soft soil area[J]. Building Structure, 2021, 51(10): 128-134.
- [2] Chen F Q, Su F. Numerical analysis of influence of foundation pit excavation on ultimate bearing capacity of adjacent foundation[J]. Journal of Disaster Prevention and Mitigation Engineering, 2008, (04): 468-472+483.
- [3] Qin H G. Deformation monitoring and analysis of foundation pit excavation on adjacent buildings[J]. Science and Technology Innovation Herald, 2020, 17(05): 36-37.

- [4] Li D P, Yan C H, Zhang S. Research progress on influence of deep foundation pit excavation on surrounding environment[J]. Engineering Journal of Wuhan University, 2018, 51(08): 659-668.
- [5] Zheng G, Zhu H H, Liu X R, et al. Safety and environmental impact control of excavation engineering and underground engineering[J]. China Civil Engineering Journal, 2016, 49(06): 1-24.
- [6] Shui W H. Study on deformation behavior of deep foundation pit excavation in loess site[D]. Xi'an University of Architecture and Technology, 2001.
- [7] Sun J H, Li Q Y. Numerical Analysis of the Excavation of Deep Pit Based on Mohr-Coulomb Failure Model[J]. Advanced Materials Research, 2014, 3149(919-921): 697-700.
- [8] Wang H Y, Yang M, Wang W. Numerical simulation of reduction behavior of bearing capacity of strip foundation adjacent to foundation pit[J]. Industrial Construction, 2006, (06): 54-58.
- [9] Shi G, Wang J G, Zhi X L, et al. Zonal calculation method for subgrade bearing capacity of highway engineering in loess region[J]. Journal of Traffic and Transportation Engineering, 2005, (04): 48-52.
- [10] Liu Y L, Shi G, Zhi X L. Study on zoning of subgrade bearing capacity in loess region[J]. Journal of Highway and Transportation Research and Development, 2005, (09): 12-15.
- [11] Wang X J, Mu N S, Wu Q. Statistical characteristics of physical and mechanical property indexes of new loess[J]. Highway Engineering, 2014, 39(01): 88-93.
- [12] Fan Z J. Overall stability analysis of foundation pit support[J]. Transpo World, 2013, (06): 203-204.
- [13] Sheng Z Q, Cui T. Engineering characteristics of foundation soil under unloading stress path of foundation pit excavation[J]. Building Science, 2018, 34(07): 1-11.
- [14] Xu F J, Tan J H. Study on comprehensive characteristics of deep foundation pit excavation with diaphragm wall[J]. Chinese Journal of Geotechnical Engineering, 1993, (06): 28-33.
- [15] Wang L. Study on optimization of support structure for deep foundation pit in collapsible loess[D]. Taiyuan University of Technology, 2004.
- [16] Du T. Deformation law and stability analysis of narrow and long deep foundation pit for subway[D]. Beijing Jiaotong University, 2012.
- [17] Cheng G Y, Wang Z Y, Liu D H. Further discussion on Terzaghi's coefficients of ultimate bearing capacity[J]. Journal of Civil Aviation University of China, 2022, 40(02): 52-57.
- [18] Meng D Y, Wu Y P. Determination and correction of subgrade bearing capacity[J]. West-China Exploration Engineering, 2009, 21(07): 42-45.
- [19] Li Y. Discussion on influence of foundation pit excavation on bearing capacity of adjacent buildings foundation[J]. Shanxi Architecture, 2005, (14): 74-75.
- [20] Cao L J, Wang Y C, Du M Z. Finite element analysis of influence of foundation pit excavation and dewatering on adjacent tunnel[J]. Occupancy, 2025, (08): 70-72.
- [21] Li H H, Lai X Y. Deformation monitoring and numerical simulation of a deep large foundation pit project in Hangzhou[J]. Soil Engineering and Foundation, 2023, 37(03): 395-401.
- [22] Tu S Y, Zeng Y, Yin S Q, et al. Study on ultimate bearing capacity of heterogeneous layered foundation[J]. Building Structure, 2021, 51(S1): 1857-1861.